Journal Pre-proofs

Magnetic parameters as proxies for anthropogenic pollution in water reservoir sediments from Mexico: an interdisciplinary approach

Marcos A.E. Chaparro, Margarita Ramírez-Ramírez, Mauro A.E. Chaparro, Raúl Miranda-Avilés, María J. Puy-Alquiza, Harald N. Böhnel, Gabriela A. Zanor

PII: S0048-9697(19)34334-7
DOI: https://doi.org/10.1016/j.scitotenv.2019.134343
Reference: STOTEN 134343

To appear in: *Science of the Total Environment*

Received Date: 10 July 2019
Revised Date: 6 September 2019
Accepted Date: 6 September 2019

Please cite this article as: M.A.E. Chaparro, M. Ramírez-Ramírez, M.A.E. Chaparro, R. Miranda-Avilés, M.J. Puy-Alquiza, H.N. Böhnel, G.A. Zanor, Magnetic parameters as proxies for anthropogenic pollution in water reservoir sediments from Mexico: an interdisciplinary approach, *Science of the Total Environment* (2019), doi: https://doi.org/10.1016/j.scitotenv.2019.134343

Magnetic parameters as proxies for anthropogenic pollution in water reservoir sediments from Mexico: an interdisciplinary approach

Marcos A.E. Chaparro[a], Margarita Ramírez-Ramírez[b], Mauro A.E. Chaparro[c], Raúl Miranda-Avilés[d], María J. Puy-Alquiza[d], Harald N. Böhnel[e], Gabriela A. Zanor[b,*]

[a] Centro de Investigaciones en Física e Ingeniería del Centro de la Provincia de Buenos Aires (CIFICEN, CONICET-UNCPBA), Pinto 399, 7000 Tandil, Argentina. chapator@exa.unicen.edu.ar (ORCID ID: 0000-0003-2832-2151).

[b] División de Ciencias de la Vida (DICIVA, Universidad de Guanajuato). gzanor@ugto.mx; margarita20_17ramirez@outlook.com

[c] Centro Marplatense de Investigaciones Matemáticas (CEMIM-UNMDP-CONICET), Diagonal J. B. Alberdi 2695, Mar del Plata, Argentina. chaparromauro76@gmail.com

[d] Departamento de Ingeniería en Minas, Metalurgia y Geología. Universidad de Guanajuato. rmiranda66@gmail.com; yosune.puy155@gmail.com

[e] Centro de Geociencias - UNAM, Boulevard Juriquilla No. 3001, 76230 Querétaro, México. hboehnel@geociencias.unam.mx

[*]Name and contact detail of the corresponding author:
Gabriela A. Zanor. División de Ciencias de la Vida (DICIVA), Campus Irapuato-Salamanca, Universidad de Guanajuato, Carretera Irapuato-Silao Km 9, C.P. 36500, Irapuato, México.
Email: gzanor@ugto.mx
ORCID ID: 0000-0002-2694-3571

Abstract

We assess the element pollution level of water reservoir sediments using environmental magnetism techniques as a novel approach. Although "La Purísima" Water Reservoir is an important source for multiple activities (e.g. recreational, fishing and agricultural) in Guanajuato state, it has been receiving for the last centuries a high load of pollutants by mining extraction, urbanization and land-use change from the Guanajuato Hydrological Basin. The analyses of environmental magnetism, geochemistry, X-ray energy dispersive spectroscopy, scanning electron microscopy and multivariate methods were applied to study sediments from the reservoir and basin. Accordingly, they indicate the presence of iron oxides (magnetite and hematite) and iron sulfides (pyrite and greigite), which evidences relevant differences in particle size and concentration within the water reservoir (median mass-specific magnetic susceptibility $\chi = 23.2\times10^{-8}$ m^3/kg), as well as with respect to the river basin sediments (median $\chi = 88.8\times10^{-8}$ m^3/kg). The highest enrichment factor EF values (median values of EF = 2–10 for As, Co, Ba, Cu, Cd, Ni and EF > 20 for S) are mainly associated with historical mining activities that have led to an enrichment of potentially toxic elements on these water reservoir sediments. We propose the use of concentration and grain size dependent magnetic parameters, i.e. χ, remanent magnetizations and anhysteretic ratios ARM/SIRM and χ_{ARM}/χ, as proxies for Ba, Co, Cr, Ni, P and Pb pollution in these river and water reservoir sediments. Such parameters allow to evaluate this sedimentary environment, and similar ones, through useful and convenient proxies.

Keywords: enrichment factor EF; magnetic proxies; mining; multivariate statistics; reservoir sediments

1. Introduction

In the planet there are numerous types of lakes that have different natural origins (tectonic, glacial, volcanic, aeolian, fluvial, etc.) and anthropogenic lakes (reservoirs; Wetzel, 2001). Lacustrine systems are subjected to the effects of external and internal factors, such as, climate, basin hydrology, vegetation cover and land use (Cohen, 2003). Lakes are one of the most sensitive continental environments which response to natural and anthropogenic forcing agents through physical, chemical and biological changes, which are recorded in their sediments (sedimentary facies, geochemistry, microorganisms). These characteristics in sediment materials constitute indirect indicators or proxies that allow to study the ecosystem dynamics, sedimentary processes and main pollution sources (Fritz, 1996). According to Zahra et al. (2014), organic and inorganic pollutants (heavy metals) are mainly introduced into the aquatic systems through point sources such as industrial, municipal and domestic wastewater effluents as well as diffuse inputs which include surface runoff, erosion and atmospheric deposition.

Environmental magnetism is an interdisciplinary subject that integrates research on a wide range of topics (Evans and Heller, 2003). It has grown considerably in the last four decades contributing to investigate different issues of climate change, pollution, iron biomineralization, and depositional and diagenetic processes in sediments applications (Liu et al., 2012). The environmental magnetic approach can briefly be summarized as the investigation of magnetic mineralogy in natural and anthropogenic samples by measurement of both their induced and remanent magnetization responses when exposed to magnetic fields. The speed of magnetic measurements, compared with other types of mineralogical analysis, and their nondestructive nature, enables measurement of large numbers of samples, a key advantage in obtaining high resolution (spatial and/or temporal) environmental data (Gubbins and Herrero-Bervera, 2007).

A number of magnetic parameters, such as magnetic susceptibility, remanent magnetization, remanent coercivity, anhysteretic ratios, etc., is often measured/calculated in

environmental magnetism, and they vary according to the concentration, mineralogy and grain size of the magnetic minerals present in specimens. The use of these magnetic parameters as proxy for pollution is possible considering the following points: a) the magnetic contribution associated with the anthropogenic activities must be distinctive from the background contribution of natural magnetic sources; b) relationships between the magnetic properties and contaminants have to be established; and c) processes affecting particle transport and deposition, as well as postdepositional changes, can be significant (Maher and Thompson, 1999). Although magnetic susceptibility proved to be a one of the best proxy for contamination in a large number of studies, other magnetic parameters have been investigated as indicators of anthropogenic pollution (Chaparro et al., 2006). The relationship between magnetic parameters and potentially toxic elements (PTE) may not be generalized for all environments, i.e. soils, rivers, lakes, urban areas, etc., and therefore this nature has to be explored in detail before using different magnetic parameters as pollution proxies (Chaparro et al., 2015b, Mejía-Echeverry et al., 2018). Among others, Chaparro et al. (2011, 2012) analyzed the nature and relationship between different variables using multivariate analyses and fuzzy tools for magnetic monitoring in soils, stream and river sediments. Magnetism studies applied in different continental and marine environments (Petrovský et al., 1998; Desenfant et al., 2004; Yang et al., 2007; Franke et al., 2009; Horng et al., 2009; Zhang et al., 2012; Chaparro et al., 2015a, Pan et al., 2019, Sepúlveda et al., 2019) indicate that this methodology combined with geochemistry (sediment quality indicators; Duodu et al., 2016) and other traditional techniques is an effective tool for assessing the PTE pollution levels recorded in sediments.

The Lerma-Chapala basin is one of the largest hydrological systems in central Mexico (54,448 km^2) that concentrates 12.6 million inhabitants with a high economic development. However, in this region there is a great concern about the impact of anthropogenic activities on water resources (Metcalfe and O'Hara, 1992; Ávila-Pérez et al., 1999; Gutierrez et al., 2009; Espinal-Carreón et al., 2013). Special attention is placed on numerous reservoirs because their freshwater is used for agricultural irrigation, fishing and as a source for drinking water.

Particularly, "La Purísima" water reservoir (PWR; Natural Protected Area: 27 km^2) belongs to the Guanajuato Hydrological Basin (GHB; Fig. 1), which forms part of the Lerma-Chapala drainage basin and its dam is the second largest in the Guanajuato state. This water body was built between 1978 and 1979 and since its construction, it has been providing water to irrigate a vast agricultural area, acting as a recharge for aquifers and allowing fishing activities. This ecosystem fulfills multiple ecological, social and economic functions, but in the last decades this reservoir has been strongly impacted by mining, urbanization, domestic wastewater discharges and agriculture development from the catchment area. Cano et al. (2000) studied the contents of metal(oid)s in five water and sediment samples of La Purísima reservoir and they found that As, Pb, Hg and Se, especially in water, overpass the quality standard for aquatic life (25, 30, 80 and 180 times, respectively). Indeed, pollution by trace metals from the Guanajuato Mining District (GMD), a region that concentrates the principal mineral deposits of the catchment area (Mother Lode: Carrillo-Chávez et al., 2003; Fig. 1), was reported by Ramos-Arroyo and Siebe-Grabach (2006) and Miranda-Avilés et al. (2012). These authors identified a serious pollution problem in the region due to historical discharges of mine tailings (since 1500s). According with the production history, approximately 95 million tons of mineralized rock have been extracted and processed by different methods: smelting and amalgamation (from 1548 to 1905), cyanidation (from 1905 to present), and flotation (from 1946 to present). Some elements present in the tailings (As, Cd, Cu, Pb, Se, and Zn, in addition to Hg and cyanide, which were added during processing) were released and mobilized into the basin, affecting the quality of water and sediments (Ramos-Ramírez, 1991; Mendoza et al., 2006; Miranda-Avilés et al., 2009).

In this study, we assess the pollution level on these sediments using environmental magnetism techniques as a novel approach, together with geochemistry and multivariate techniques. The specific objectives are: i) to determine the magnetic properties of sediments from GHB and PWR; ii) to determine concentrations of PTE in sediments, calculate the Enrichment Factor (EF) for each element and the Index of Pollution (PLI) using a regional

background and comparing GHB and PWR sediments; iii) to analyze the relationships between magnetic parameters and PTE, and iv) to determine the relevant magnetic parameters as proxies for PTE pollution, which allows to evaluate the spatial distribution of pollutants. Finally, this research is expected to provide useful information about the potential environmental risk associated with the presence of toxic elements in a water reservoir in central Mexico.

2. Materials and methods

2.1. Study area

La Purísima water reservoir is located in the Guanajuato state, central Mexico (20°52'41"N; 101°16'47"W; 1850 m a.s.l.; Fig. 1). It is part of the Lerma-Santiago hydrological basin, one of the more extensive and populated in the country. This reservoir is part of the hydrological sub-basin which is called Guanajuato Hydrological Basin (area: 500 km^2; Fig. 1). La Purísima has an area of about 8.5 km^2 with an elongated shape and a maximum water depth of 26 m, increasing from riverine through transitional to lacustrine zones next to the dam. Waters from PWR are neutral to alkaline, with pH values varying between 7.0 and 8.7 (mean of 8.2). The water reservoir was built between 1978 and 1979 (capacity: 110 Mm^3) with the main purposes of agricultural irrigation, flooding control and as a recharge for regional and local aquifers of the catchment area. Land uses in the region are mining, agriculture and urbanization (Fig. 1).

According to the geological map from the Servicio Geológico Mexicano (SGM), the main lithology is composed of acid and basic igneous rocks (ignimbrite-rhyolite and andesite-basalt, respectively) of Tertiary age. The area is also characterized by modern sedimentary rocks and sediments, including Tertiary conglomerates and Quaternary alluvial deposits. Regional rainfall averages 580 mm/year (period 1979-2014) and evapotranspiration reaches a total annual value of 2325 mm (data source: Servicio Meteorológico Nacional, SMN). A maximum mean temperature of about 23 °C is registered in May while the minimum mean temperature corresponds to January with 15.1 °C. The reservoir water level rises during the rainy-warm season (June-September) and drops during the dry-warm season (March-May).

2.2. Sampling, physico-chemical analysis and available data

The sampling campaign was carried out in seventeen sites within the PWR, and in twelve sites in the GHB (Fig. 1). In this reservoir, bottom sediments were collected using an Ekman dredger in January-September 2017, samples P1/4/6/10/12/13/14/15/16/17/18/19/21/22/23 and R1/2. Sediments in the hydrological basin were taken in the river's beds, using a plastic shovel, and they were labeled as samples CLM-001/003/007/009/010/014/015/016/017/018/020/021. The collected sediments were placed in polyethylene bags and were dried at room temperature in open air for a couple of days in the Environmental Geology Laboratory (División de Ciencias de la Vida, Universidad de Guanajuato). Dry material was quartered and sieved (2-mm) to remove coarse fraction, and then they were packed and stored in polyethylene bags for measurements.

The particle size fractions (sand, silt and clay) were determined using an hydrometer (Bouyoucos, 1962). First, sediment samples were pre-treated with 10% HCl and 30% H_2O_2 to eliminate carbonates and organic matter, respectively. Organic carbon contents were quantified by Loss On Ignition (LOI; Heiri et al., 2001), at 550 °C for 3 h.

Available elemental data of the hydrological basin provided by the Servicio Geológico Mexicano (2017) were used in this work. Such 14 data were labeled as SGM-11/12/14/15/16/20/21/22/23/744/745/751/752/753 and correspond to contents of As, Ba, Be, Cd, Co, Cr, Cu, Fe, Mg, Mn, Ni, P, Pb, and Zn, which are detailed in Table 1.

2.3. Magnetic measurements

The environmental magnetism measurements were carried out in the laboratory of Paleomagnetism and Environmental Magnetism at the CIFICEN (UNCPBA, Argentina) and in the laboratory of Paleomagnetism and Rock Magnetism at the Centro de Geociencias (UNAM, México). The air dried sediments were sub sampled for magnetism studies using plastic containers (about 2.3 cm^3), and special containers holding ~20 and 100 mg of material for magnetic hysteresis and thermomagnetic measurements, respectively. Prior to remanent

magnetization measurements, all samples were fixed using sodium silicate to prevent unwanted movement of particles.

A total of 29 samples (GHB: n=12; PWR: n=17) were analyzed for magnetic susceptibility, ARM and IRM measurements. A reduced number of samples for GHB: n=3 and PWR: n=5 were analyzed by magnetic hysteresis; as well as 12 samples (GHB: n=3 and PWR: n=9) for thermomagnetic measurements.

Magnetic susceptibility measurements were made using the magnetic susceptibility meter MS2 (Bartington Instruments Ltd.) linked to the MS2B dual frequency sensor (0.47 and 4.7 KHz). These measurements were done on the higher sensitivity range (0.1 x 10-5 SI); and they were corrected for drift through five measurement cycles (two air readings and three sample readings). The accuracy of the magnetic susceptibility measurement is 1%. The mass-specific susceptibility (χ), frequency dependent magnetic susceptibility χ_{fd} were calculated. The anhysteretic remanent magnetization (ARM) was imparted using a device attached to a shielded demagnetizer (Molspin Ltd.), superimposing a DC bias field of 90 μT (71.6 A/m) to a peak alternating field (AF) of 100 mT, and an AF decay rate of 17 μT per cycle. The remanent magnetization was measured with a spinner fluxgate magnetometer (Minispin, Molspin Ltd.). Mass-specific anhysteretic susceptibility (χ_{ARM}) was calculated using linear regression for ARM acquired at two DC bias fields of 50 and 90 μT (39.8 and 71.6 A/m). The anhysteretic ratio χ_{ARM}/χ, was also calculated. The isothermal remanent magnetization acquisition (IRM) studies were performed using a pulse magnetizer model IM-10-30 (ASC Scientific). Each sample was magnetized by exposing it to stepwise incrementing DC fields, from 1.7 mT to 2470 mT. The remanent magnetization after each step was measured using the above-mentioned Minispin magnetometer. In these measurements, IRM acquisition curves, the remanent acquisition coercivity ($H_{1/2}$), and the saturation of IRM (SIRM= IRM_{2470mT}) were determined using forward DC fields. Magnetic hysteresis measurements were carried out using a MicroMag™ 2900 magnetometer (Alternating Gradient Magnetometer, Princeton Measurements Corporation). Related magnetic parameters were determined from these measurements: saturation

magnetization (M_s), remanent saturation magnetization (M_r), relative contribution of paramagnetic minerals to the M_s (Paramag. Cont.), coercivity field (H_c) and remanent coercivity (H_{cr}). The temperature dependence of high-field magnetization measurements were carried out using a laboratory-made horizontal magnetic translation balance. The magnetic field was 0.5 T, the temperature was controlled and the force compensated and recorded with a sensor that generates an output voltage. Such voltage is recorded using a PicoLog® recorder. Measurements were performed in air, and each sample was heated to a temperature of about 700 °C and then cooled to room temperature (RT) with a controlled heating/cooling rate of 30 °C/ min.

The readers unfamiliar with environmental magnetism methods and techniques are addressed to consult the practical guides reported by Walden et al. (1999) and Dearing (1999).

2.4. Geochemical analyses and pollution indices

Near-total concentrations of As, B, Ba, Be, Cd, Co, Cr, Cu, Fe, Mg, Mn, Ni, P, Pb, S, V, and Zn in the sediments (n= 17) were determined in the Laboratory of Water Geochemistry at Centro de Geociencias (CGEO-UNAM) by Inductively Coupled Plasma Atomic Emission Spectroscopy (ICP-OES), following the method 6010C by U.S. EPA (2000). Sediment samples were digested following the method 3051 (U.S. EPA, 2007). Sediments weighted 0.5 g were treated with 10 mL of ultrapure HNO_3 (JTBaker), using a microwave oven CEM (MARS Xpress) which operated at one ramp (1600 watt), at 120°C for 15 min (holding time: 15 min). The accuracy of the results was checked against measurement of an internal blank, a sample prepared with a high purity certified standard (QCS-26) and one standard reference material (NIST 2710A).

Two pollution indices were calculated for both PWR (n= 17) and GHB (n= 14) samples. The enrichment factor EF defined by Szefer (1998) was calculated for each sample and element concentration (x) using the equation $EF^x_{Al} = (x/Fe)_{sample} / (x/Fe)_{background}$. According to Sutherland

(2000), five categories are proposed as minimum (EF < 2), moderate (EF = 2–5), significant (EF = 5–20), very high (EF = 20–40) and extremely high enrichment (EF > 40).

On the other hand, the pollution index (PLI, Tomlinson et al., 1980), a composite index based on thirteen PTE: As, Ba, Be, Cd, Co, Cr, Cu, Mg, Mn, Ni, P, Pb and Zn was calculated using the equation: $PLI = \sqrt[n]{\prod_{i=1}^{n}(C_{HM,i} / C_{background,i})}$; where $C_{HM,i}$ is the concentration of each element, and $C_{background,i}$ is the background value for each element.

In this work, the background values were calculated using 14 data from GHB provided by the Servicio Geológico Mexicano (2017, Table 1) and the iterative 2-δ technique by Matschullat et al. (2000), except for B, S, and V that correspond to the upper continental crust data (UCC, Rudnick and Gao, 2003).

2.5. X-ray energy dispersive spectroscopy and scanning electron microscopy

The morphology and elemental composition of sediments were also studied in the Laboratory of Centro de Geociencias and at the Laboratorio de Investigación y Caracterización de Minerales (Universidad de Guanajuato, México) using magnetic extracts for various sediment samples. Particles were identified by a Phillips model XL30 scanning electron microscopy (SEM). This microscope also allowed to analyze the elemental composition of each specimen by X-ray energy dispersive spectroscopy (EDS) with an EDAX model DX4 (detection limit 0.5%).

2.6. Statistical methods

Prior to multivariate analyses, descriptive statistics for magnetic and elemental variables were studied. Multivariate analyses were performed using the R free software: R version 3.4.0 (R Core Team, 2017). The relationships between variables were analyzed by principal component analysis (PCA) with matrix correlation; and after this analysis, a non-hierarchical k-means clustering (CA) with Euclidean distance was performed. The coordinates of the rows obtained from PCA were used to build the clusters. All PWR (n = 17) and some GHB (n = 5)

samples, and a total of 20 variables were used for these analyses. In particular, the magnetic variables were: χ, SIRM, ARM, χ_{ARM}/χ, ARM/SIRM and SIRM/χ; and EF variables: EF_{As}, EF_{Ba}, EF_{Be}, EF_{Cd}, EF_{Co}, EF_{Cr}, EF_{Cu}, EF_{Mg}, EF_{Mn}, EF_{Ni}, EF_{P}, EF_{Pb}, EF_{S} and EF_{Zn}.

The spatial distribution of χ and ARM/SIRM in the water reservoir was represented in a prediction map, which was built through a geostatistical analysis, i.e. the ordinary kriging method (OKM). The OKM is one of the most popular interpolation spatial method because it considers knowledge of the spatial variation as represented in the variogram function, and do not require additional information than the measurement values and their geographic coordinates. The spatial continuity and statistical assumptions were verified.

3. Results

3.1. Elemental concentrations, grain size, LOI550 contents and magnetic minerals

Magnetic parameters and elemental contents evidence differences between sampling sites and between PWR and GHB sediments. Such differences can be appreciated in Table 1 and Table 2.

All elements for PWR sediments have higher median contents than GHB sediments (Fig. 2), such values for PWR are 13.2 mg/kg (As), 28.0 mg/kg (B), 256.7 mg/kg (Ba), 1.8 mg/kg (Be), 1.5 mg/kg (Cd), 11.6 mg/kg (Co), 42.6 mg/kg (Cr), 30.0 mg/kg (Cu), 28753 mg/kg (Fe), 10567 mg/kg (Mg), 784 mg/kg (Mn), 17.8 mg/kg (Ni), 723 mg/kg (P), 28.6 mg/kg (Pb), 1.8 mg/kg (Be), 7146 mg/kg (S), 98.4 mg/kg (V), 1.8 mg/kg (Be), 91.7 mg/kg (Zn), and 2.2 (PLI), reaching increments of 12–207% with respect to GHB sediments.

Grain size in PWR sediments is fine, with a dominant silty fraction (61.8-89.8%; Table 2). Clay contents vary from 6 to 18% while sand contents show values between 2 and 24.2%. There is not a spatial pattern of grain size distribution between different zones into the reservoir. On the other hand, LOI550 contents show a spatial pattern with higher values in sediments located in deep water zones (P10, 13, 14, 15, 17, 19 and 23; min-max values = 9.5–14.6%) than in littoral

areas (P6, 12, 16, 18, 21 and 22; min-max values = 8.8–13.5%), and in riverine/littoral areas (P1, P4, R1 and R2; min-max values = 6.2–8.3%; Table 2).

Sediments from GHB, sample CLM-007, have a low coercivity component ($H_{1/2}$= 57.5 mT) with a high contribution of 81%, and a high coercivity component ($H_{1/2}$= 234.4 mT) with a low contribution (13%). The acquisition IRM measurements for reservoir sediments, samples P15, and P19, show two main magnetic phases (Fig. 3). On one hand, a ferrimagnetic mineral component with a contribution to the SIRM of 71–79% characterized by low coercivity ($H_{1/2}$= 44.7–52.5 mT) such as magnetite-like minerals, and on the other hand a high coercivity component ($H_{1/2}$= 389.0–457.1 mT) with a low contribution (17–25%) corresponding to reported remanent acquisition coercivity values of hematite minerals, which ranges between 28 and 769 mT with an average value of 270 mT (Peters and Dekkers, 2003).

The thermomagnetic and magnetic hysteresis results confirm the presence of magnetite as a main carrier for these sediments (H_c= 12.5–18.9 mT and H_{cr}= 40.0–49.6 mT for GHB sediment samples; and H_c= 7.3–17.8 mT and H_{cr}= 37.4–49.2 mT for PWR sediments samples, Table 1). As observed from magnetic hysteresis loops (Fig. 4b, 4d, 4f), the contribution of paramagnetic minerals is a distinctive characteristic between both environments, sediments within the reservoir have higher paramagnetic mineral contents (Paramag. Cont.= 36.1–186.8%) than river sediments from the catchment (Paramag. Cont.= 8.1–15.5%, Table 1).

Such distinctive difference is evident from thermomagnetic measurements, which showed a linear decrease in magnetization up to 400°C only for PWR sediments, reaching a 25–35% of M_{RT} and a subsequent increase between 400°C and 500°C that is indicative of iron sulfides minerals such as pyrite (FeS_2) and greigite (Fe_3S_4, Roberts et al. 2011). This magnetic transformation (a pronounced peak) is better expressed in the following order, the deepest PWR areas (sample P15, Fig. 4c), deep water areas (P10, and P21), littoral areas (P4), and Guanajuato and Chapin river mouths (sample R2, Fig. 4a). On the other hand, there is another decrease in magnetization at 550–580°C observed in both PWR and GHB sediments, which is characteristic of (titano)magnetite mineral.

Smaller ferrimagnetic particles are observed in the deepest water levels of PWR by analyzing magnetic particle size dependent parameters (χ_{ARM}/χ and ARM/SIRM). Values of anhysteretic ratios are higher (smaller particles) in deep water areas (χ_{ARM}/χ= 8.9–10.1, and ARM/SIRM= 0.045–0.054, for sites P14, P19 and P23) than in littoral and river mouth areas (χ_{ARM}/χ= 4.8–5.1, and ARM/SIRM= 0.015–0.022, for sites P1, R1 and R2). A general comparison between the river basin and the reservoir shows coarser magnetic particles in the source, i.e. GHB sediments (median χ_{ARM}/χ= 2.9, and median ARM/SIRM= 0.013), than in the deposition area PWR (median χ_{ARM}/χ= 6.2, and median ARM/SIRM= 0.034; Table 1).

Concentration dependent magnetic parameters, i.e. χ, ARM and SIRM, vary widely along the basin, e.g.: χ= 36.7–391.2 $\times10^{-8}$ m^3/kg and SIRM= 7.1–44.3 $\times10^{-3}Am^2/kg$ (Table 1). There is a distinctive magnetic behavior between sediment source (i.e. GHB) and sedimentary deposition (i.e. PWR); sediments from GHB have higher values (median χ= 88.8 $\times10^{-8}m^3/kg$) than sediments from the PWR (median χ= 23.2 $\times10^{-8}m^3/kg$ Table 1). Concentration of ferrimagnetic minerals is four-fold higher for GHB (e.g. median SIRM= 14.7 $\times10^{-3}Am^2/kg$) than PWR (e.g. median SIRM= 4.2 $\times10^{-3}Am^2/kg$) sediments.

3.2. SEM observations

The observation by SEM-EDS confirmed the presence of magnetite, pyrite and greigite minerals that are displayed in Fig. 5. Although in samples from both deep water (P14) and littoral (P1) areas are (titano)magnetite minerals (e.g. Fig. 5d, 5e, 5f), the deep water areas (P14) evidence the formation of iron sulfides from piritization reactions, which is possible in anoxic sulfate-reducing sedimentary environments.

Spherical framboids with variable diameters of 6–25 μm were observed, composition by EDS of individual crystals corresponds to pyrite crystals with atomic molar ratios of Fe to S that varied between 0.50 and 0.55. Individual cubo-octahedral crystals (coarser-grained) of pyrite of 1–1.5μm and finer particles ranging from 0.3–0.5 μm (possibly greigite crystals) are appreciated in Fig. 5a, 5c, 5e.

3.3. Enrichment factor, pollution index and multivariate analysis

The adverse impact of elements in PWR sediments were analyzed using the enrichment factor EF and the pollution index PLI. Most elements for PWR samples have median values of EF < 2 (minimum enrichment); except As, Ba, Cd, Ni and S (with EFs of 2.0, 2.7, 2.7, 3.4 and 83.5; i.e. moderate and extremely high enrichment, respectively). Higher median values are observed for GHB compared to PWR samples, only for elements Co, Cr, Cu, Ni and Pb (EFs of 6.3, 1.6, 2.2, 9.3 and 1.9, respectively). In addition, the composite index PLI based on PTE gives median values of 2.2 and 1.9 for PWR and GHB samples, respectively. This index indicates how much a sample exceeds the contents of elements for an uncontaminated environment, which has a reference PLI value of 1. The PLI gives an assessment of the overall pollution status for a sample, and it is a result of the contribution of several PTE. These results can be appreciated in Fig. 6.

The principal components analysis with correlation matrix shows the relationships between magnetic and geochemical variables, and the first three principal components (PC) accounted for a 70.6% of the total variance (Fig. 7a). Ten out of twenty variables contribute to the first component (PC1), which are χ, SIRM, χ_{ARM}/χ, ARM/SIRM, EF_{Ba}, EF_{Co}, EF_{Cr}, EF_{Ni}, EF_{P} and EF_{Pb}. The concentration dependent magnetic parameters (χ and SIRM) are directly correlated with the enrichment of Co, Cr, Ni, and Pb. On the other hand, the grain size dependent magnetic parameters (χ_{ARM}/χ, ARM/SIRM) correlate directly with the enrichment of Ba and P. Six out of twenty variables contribute to PC2 (ARM, SIRM/χ, EF_{Mn} and EF_{S}) and PC3 (EF_{Cd} and EF_{Zn}) as observed in Fig. 7a. On the other hand, the analysis of magnetic parameters with LOI550, sand, silt and clay contents shows that χ, SIRM, ARM, χ_{fd}, ARM/SIRM and LOI550 contribute to PC1, and sand, silt and clay to PC2. As observed in Fig. I and Table II (Supp. Data), LOI550 is directly correlated with ARM/SIRM; and inversely correlated with χ, SIRM, χ_{fd} and ARM.

Differences between PWR and GHB samples were confirmed by performing a cluster analysis using the first five PCs; which retained >90% of the data variance and were used to

build the clusters. This very high percentage of the inertia retained by selected PCs allows to obtain a stable and clear hierarchy. Three clusters are the optimal partition of samples, the first two clusters, as observed in Fig. 7b, are made of twelve PWR samples (cluster 1: P10, P12, P13, P14, P15, P16, P17, P18, P19, P21, P22 and P23) and seven PWR and GHB samples (cluster 2: P1, P4, P6, R1, R2, CLM-017 and CLM-020). Cluster 1 comprises only samples from the water reservoir, and cluster 2 is made of "transitional" areas, such as littoral PWR sites (P1, P4 and P6), river mouths (R1 and R2) and river samples (CLM-017 and CLM-020) close to the water reservoir (Fig. 1). The third grouping (cluster 3) is made of three GHB samples (CLM-007. CLM-009 and CLM-010).

4. Discussion

4.1. Magnetic properties and pollution levels within PWR

Magnetic properties of GHB and PWR sediments indicate the presence of (titano)magnetite as the main ferrimagnetic carrier, hematite is also detected but its contribution is lower than ferrimagnetic minerals. As expected for a sediment deposition area, sizes of ferrimagnetic iron oxides estimated from anhysteretic ratios (χ_{ARM}/χ, and ARM/SIRM) are smaller in the water reservoir than in the hydrological basin, thus favoring the sediment adsorption of potentially toxic elements, as reported in river sediments (Chaparro et al., 2004), in intertidal sediments (Zhang et al., 2007) and in estuarine sediments (Dessai et al., 2009), among others. Rose and Bianchi-Mosquera (1993) studied the adsorption of several elements onto goethite and hematite, finding that, under oxidizing conditions at 25°C and at a pH greater than 6, the metals are adsorbed in the order Cu > Pb > Zn > Co > Ni > Ag with increasing pH, and this order changes to Pb > Zn > Co > Ni > Cu under reducing conditions (Fe^{2+}-goethite). Recently, Lasheen et al. (2015) studied nano magnetite and its composite with kaolinite for Cu, Pb, Cd, Cr, and Ni adsorption. They proved that the adsorption capacity (of metal ions from aqueous solutions) of the magnetic composite increased with time and with higher pH. The adsorption capacities of metal in that study followed the order: Cu > Pb > Cr > Cd > Ni.

Furthermore, in this study, dominant finer fractions and high LOI550 contents in the deepest zone of the reservoir, which are directly correlated with ARM/SIRM (Table II, Supp. Data) contribute to enhance the adsorption of heavy metals onto these sediments, as it was also observed by Zahra et al. (2014).

Although paramagnetic minerals such as pyrite evidence an important contribution within the water reservoir from magnetic hysteresis (Paramag. Cont. up to 190%, Table 2) and thermomagnetic measurements, the contrary occurs for GHB sediments. It is worth of mentioning that SEM-EDS studies support this magnetic analysis, showing the presence of characteristic spherical framboids (6–25 μm in diameter) composed of individual cubo-octahedral crystals of pyrite (coarser-grained) and finer particles (0.3-0.5 μm) of possibly greigite crystals, which are well known to form as precursors to pyrite in such environments (Roberts et al., 2011). Differences between sediments are also exhibited by mass-specific magnetic susceptibility values that decrease from GHB sediments (median χ= 88.8 $\times 10^{-8}$ m^3/kg) to PWR sediments (median χ= 23.2$\times 10^{-8}$ m^3/kg). Moreover, in PWR, magnetic concentration parameters decrease from littoral sites ($\chi \approx$ 60 $\times 10^{-8} m^3/kg$) to deep water areas ($\chi \approx$ 20 $\times 10^{-8} m^3/kg$) within the water reservoir. Reported χ values of magnetite ferrimagnetic mineral (0.4–1.1 $\times 10^{-3}$ m^3/kg) are approximately a thousand times greater than that of pyrite paramagnetic mineral (0.3 $\times 10^{-6}$ m^3/kg; Dearing, 1999). In addition, the pyrite mineral contents increase from littoral to deep water areas in the water reservoir; the deepest areas (lacustrine zones) reach about 26 m and provide alkaline, anoxic and sulfate-reducing sedimentary sub-environments where piritization reactions and dissolution of magnetite are possible to take place (Berner, 1984). In addition to neutral/alkaline waters of PWR, high contents of sulfur are present in these sediments, with a median value of 7146 mg/kg (Fig. 2).

Most of the element contents vary within the water reservoir, median contents of As, B, Ba, Be, Cd, Co, Cr, Cu, Fe, Mg, Mn, Ni, P, Pb, S, and Zn surpass 1.1-4.2 times the background values. According to Ramos-Arroyo et al. (2004), ~95 million tons of mineralized rock have been extracted and processed by different methods in the mining district of Guanajuato since

1548; the elements As, Cd, Cu, Pb, Se, and Zn, that were added during the extraction processing, may be hazardous because of their high toxicity. High contents (up to 2%) of sulfides and sulfosalts in Guanajuato tailings were reported by Mendoza-Amezquita et al. (2006), hence they concluded that Pb, Zn and Cu can be derived from galena (PbS), sphalerite (α-ZnS), and chalcopyrite ($CuFeS_2$), respectively. The leaching behavior of tailings from GMD, and the potential hazard of mine waste material, was evaluated geochemically by Morton-Bermea et al. (2004). They found that the trace elements V, Cr, Mn, Co, As, Se, Mo, Cd, Sb, Tl and Pb are very likely bounded to secondary minerals, which can be easily dissolved after a 10-weeks period, and hence liberated these trace elements to the catchment area. The study reported by Miranda-Avilés et al. (2012) also provided evidence that anthropogenic metals stored in the fluvial plain of Guanajuato River sub-basin represent a major potential source of pollutants to surface and groundwater in the Lerma-Santiago basin. They found that contamination of Cu, Zn, Sb, and Pb may be attributable to historical discharges of mine tailings into Guanajuato River and the use of Cu ($CuSO_4$) in the metallurgical process of amalgamation. The anthropogenic metals stored in sediments from GHB, far away from PWR, represent a major potential pollution source (Miranda-Avilés et al., 2012), which is confirmed by the element enrichments, with median values of EF < 2 and higher ones for As, Ba, Cd, Ni and S, and the PLI index (median value of 2.2) of PWR sediments in this study. In the case of Ba and V, their content could be related to the presence of some Ba-V-rich feldspars and muscovite in phyllite formations into the hydrological basin, as it was reported by Pan and Fleet (1991). Comparable values of Ni were reported in the center and north sectors of the GMD by Carrillo-Chávez et al. (2003). Finally, the high content of P in PWR may be explained by agricultural activities, as phosphorus compounds are one of the most common constituents of agrochemical additives, such as pesticides and chemical fertilizers used in agriculture. Thus, the "La Purísima" water reservoir constitutes a progressive accumulation area of pollutants.

4.2. Magnetic parameters as proxies for pollution

Magnetic proxies of pollution, such as the well-known magnetic susceptibility, have the advantage to be determined with high sensitivity combined with fast laboratory processing; sample preparation is easy, laboratory instruments are of relatively low cost, and most measurements are nondestructive (Chaparro et al., 2014). The parameter χ is perhaps the best and the most used parameter for assessing magnetic concentration in environmental samples, which is roughly proportional to the concentration of paramagnetic and ferrimagnetic minerals. SIRM and ARM are sensitive to the concentration of only ferromagnetic minerals, but ARM is also sensitive to their grain size (Dunlop and Özdemir, 1997). On the other hand, the ratios ARM/SIRM and χ_{ARM}/χ are designed to cancel the effects of magnetic mineral concentration, and enhance the signal due to variations in grain size (Liu et al., 2012). χ_{ARM}/χ is a sensitive grain size indicator of magnetite, where values of $\chi_{ARM}/\chi > 5$ are indicative of the presence of very small magnetite grains (< 1 μm). This is because χ_{ARM} is strongly grain size dependent (Peters and Dekkers, 2003).

The concentration (χ and SIRM) and grain size (ARM/SIRM and χ_{ARM}/χ) dependent magnetic parameters, organic carbon content (LOI550) and the enrichment of Ba, Co, Cr, Ni, P and Pb were identified as the variables with main contribution to the first component in PCA. Direct correlations are observed between χ, SIRM, Co, Cr, Ni and Pb; and between ARM/SIRM, χ_{ARM}/χ, Ba, P and LOI550 (Table I and II, Supp. Data). On the other hand, parameters ARM and SIRM/χ are inversely correlated with enrichment of Mn and S, which are grouped in PC2. In addition, these variables allowed to group the water reservoir and basin samples into three well-differentiated clusters. The cluster 1, made of PWR samples, is distinctively different of transitional and GHB samples grouped in cluster 2 and 3, respectively. Cluster 1 is characterized by lower mean values of concentration parameters (χ, SIRM and ARM) and enrichment of Co, Cr, Ni and Pb than the global mean, as well as higher mean values of grain size parameters (ARM/SIRM and χ_{ARM}/χ) and enrichment of Ba, Mn, S and P than the global mean. The opposite behavior for mentioned variables is observed in clusters 2 and 3.

This fact and the relationships between concentration and grain size dependent magnetic parameters and enrichment of elements support the use of parameters χ, SIRM, ARM/SIRM and χ_{ARM}/χ as proxies for Ba, Co, Cr, Ni, P and Pb pollution, and the ARM as a proxy for Mn and S pollution in GHB and PWR sediments. These magnetic proxies are proposed for this study area, and others with similar anthropogenic activities, for metal pollution monitoring in water reservoir and river sediments.

Changes in space for the magnetic proxies χ and ARM/SIRM are represented in Fig. 8. Such changes are related with characteristics of depositional (littoral and deep water) areas within the water reservoir, the input of available pollutants, and the enrichment of mentioned PTE. It is important to take into account that this representation should be considered as a geostatistical approximation because of the limited number of sampling sites.

5. Conclusions

Magnetite is the main ferrimagnetic carrier present in sediments from the river basin and the water reservoir; however, its concentration is four-fold higher for Guanajuato Hydrological Basin sediments than Purísima Water Reservoir sediments and its magnetic grain size distribution indicates the presence of fine particles in the water reservoir that favor the sediment adsorption of potentially toxic elements.

Among magnetic minerals, the iron oxide hematite, and iron sulfides pyrite and (probably) greigite are detected in PWR sediments, especially in deep water areas where early diagenesis seems to be more evident. The presence of these paramagnetic minerals within the water reservoir indicates magnetic mineral transformations through piritization reactions that have led to a decrease in magnetic concentration.

Contamination by As, Cd, Cu, Mn, S, Pb, and Zn are mainly associated to mining activities in Guanajuato Hydrological Basin which have affected the environment through historical discharges of mine tailings into the main tributaries of the Guanajuato Hydrological Basin. In contrast, Co, Cr, Ni and Ba contents in sediments may have a geogenic origin. And the

P concentrations may be explained by anthropogenic activities, such as agriculture. Purísima Water Reservoir sediments evidence moderate enrichments (median values of EF= 2–5) with respect to As, Ba, Cd, Ni and very high enrichment (median values of EF over 20) for S. On the other hand, GHB sediments evidence moderate to significant enrichment (EFs of 6.3, 1.6, 2.2, 9.3 and 1.9, respectively) only with respect to Co, Cr, Cu, Ni and Pb (EFs of 6.3, 1.6, 2.2, 9.3 and 1.9, respectively); hence, PWR and GHB sediments evidence moderate to significant enrichment.

The multivariate analyses for these sediment samples show significant differences between GHB and PWR sediments for magnetic grain size and concentration parameters and EFs variables. Differences between PWR and GHB samples were determined by cluster analysis that allows partitioning the dataset into three clusters as the optimal groups of samples. These clusters are made of sediments from deep water (cluster 1), transitional (littoral PWR sites, river mouths and river sites close to the water reservoir, cluster 2) and river basin (cluster 3) areas.

The relationships between concentration and grain size dependent magnetic parameters with PTEs allow us to use χ, SIRM, ARM/SIRM and χ_{ARM}/χ as proxies for Ba, Co, Cr, Ni, P and Pb pollution, and the ARM as a proxy for Mn and S pollution in GHB and PWR sediments. Therefore, prediction maps using these magnetic proxies provide a useful tool for future studies to evaluate and control the environmental health of water reservoirs and lakes.

Conflict of interest

There is no conflict of interest.

Acknowledgements

This contribution was supported by the Universidad de Guanajuato through project CIIC 1031/2016-2017. The authors wish to thank the Universidad de Guanajuato, the Universidad Nacional del Centro de la Provincia de Buenos Aires (UNCPBA), the Comisión Estatal del

Agua del Estado de Guanajuato (CEAG), Comisión Nacional del Agua (CONAGUA) and the National Council for Scientific and Technological Research (CONICET) for their financial support. The authors thank to both anonymous reviewers whose comments greatly improved the manuscript. They also thank Dr. M. Vega González (CGEO-UNAM) for her help in the SEM studies and to Ing. J. Escalante (CGEO-UNAM) for his help with thermomagnetic measurements.

References

Ávila-Pérez, P., Bálcazar, M., Zarazúa-Ortega, G., Barceló-Quintal, I., Díaz-Delgado, C. 1999. Heavy metal contamination in water and bottom sediments of a Mexican reservoir. The Sci. Total Environ., 234, 185-196.

Berner, R.A., 1984. Sedimentary pyrite formation: An update, Geochim. Cosmochim. Acta, 48, 605–615, doi:10.1016/0016-7037(84)90089-9.

Bouyoucos, G.J., 1962. Hydrometer method improved for making particle size analysis of soils. Agron. J., 54, 464-465.

Cano, R.I., Gómez, F.J .FV., Ramírez, V.M., Dueñas, O.F., Rodríguez, E.R., Aguilera, A. F.A., 2000. Determinación de Contaminantes en la Presa la Purísima y su efecto en el Sistema de Pozos Puentecillas de Guanajuato. In: Asignación, Productividad y Manejo de Recursos Hídricos en Cuencas, (Christopher A. Scott, Phillippus Wester y Boris Marañon-Pimentel, eds.). 123-133 pp. International Water Management Institute, Serie Latinoamericana de México #20, México y Colombo, Sri Lanka.

Carrillo-Chávez, A., Morton-Bermea, O., González-Partida, E., Rivas-Solorzano, H., Oesler, G., García-Meza, V., Hernández, E., Morale, P., Cienfuegos, E., 2003. Environmental geochemistry of the Guanajauto Mining District, Mexico. Ore Geology Reviews, 23, 277-297.

Chaparro, M.A.E., Bidegain,, J.C., Sinito, A.M., Jurado, S., Gogorza, C.S., 2004. Relevant Magnetic Parameters and Heavy Metals from Relatively Polluted Stream-sediments—Spatial

Distribution along a Crosscity Stream in Buenos Aires Province, Argentina, Stud. Geophys. Geod., 48(3), 615–636.

Chaparro, M.A.E., Gogorza, C.S.G., Chaparro, M.A.E., Irurzun, M.A., Sinito, A.M.,2006. Review of magnetism and pollution studies of various environments in Argentina. Earth Planets Space, 58 (10), 1411-1422.

Chaparro, M.A.E., Chaparro, M.A.E., Rajkumar, P., Ramasamy, V., Sinito, A.M., 2011. Magnetic parameters, trace elements and multivariate statistical studies of river sediments from south eastern India: A case study from Vellar River. Environ. Earth Sci., 63(2), 297-310.

Chaparro, M.A.E., Chaparro, M.A.E., Sinito, A.M., 2012. An interval fuzzy model for magnetic monitoring: estimation of a pollution index. Environ. Earth Sci., 66, 1477-1485.

Chaparro, M.A.E., Gargiulo, J.D., Irurzun, M.A., Chaparro, M.A.E., Lecomte, K.L., Böhnel, H.N., Córdoba, F.E., Vignoni, P.A., Manograsso-Czalbowski, N.T., Lirio, J.M., Nowaczyk, N.R., Sinito, A.M., 2014. Magnetic parameters in paleolimnological studies in Antarctica ["El uso de parámetros magnéticos en estudios paleolimnológicos en Antártida"]. Latin American Journal of Sedimentology and Basin Analysis, 21, 77–96.

Chaparro, M.A.E., Krishnamoorthy, N., Chaparro, M.A.E., Lecomte, K.L., Mullainathan, S., Mehra, R., Sinito, Ana M., 2015a. Magnetic, chemical and radionuclide studies of river sediments and their variation with different physiographic regions of Bharathapuzha River, southwestern India. Stud. Geophys. Geod., 59, 438-460.

Chaparro, M.A.E., Chaparro, M.A.E., Castañeda-Miranda, A.G., Böhnel, H.N., Sinito, A.M., 2015b. An interval fuzzy model for magnetic biomonitoring using the specie *Tillandsia recurvata* L. Ecol. Indic., 54, 238-245.

Dearing, J., 1999. Environmental magnetic susceptibility. Using the Bartington MS2 System. 2nd edn, Chi Publishing, 54 pp.

Desenfant F., Petrovský E., Rochette P., 2004. Magnetic signature of industrial pollution of stream sediments and correlation with heavy metals: case study from South France. Water Air Soil Pollut., 152(1),297–312.

Dessai, Deepti V.G., Nayak, G.N., Basavaiah, N., 2009. Grain size, geochemistry, magnetic susceptibility: Proxies in identifying sources and factors controlling distribution of metals in a tropical estuary, India. Estuar. Coast. Shelf Sci., 85 (2), 307-318.

Duodu, G.O., Goonetilleke, A., Ayoko, G.A., 2016. Comparison of pollution indices for the assessment of heavy metal in Brisbane River sediment. Environ. Pollut., 219, 1077-1091.

Espinal-Carreón, T., Sedeño-Díaz, J.E., López-López, E. Evaluación de la calidad del agua en la Laguna de Yuriria, Guanajuato, México, mediante técnicas multivariadas: un análisis de valoración para dos épocas 2005, 2009-2010. Rev. Int. Contam. Ambient., 29(3), 147-163.

Evans, M.E., Heller, F., 2003. Environmental Magnetism, Principles and Applications of Enviromagnetics. Academic Press, New York, 299 pp.

Franke C., Kissel C., Robin E., Bonté P., Lagroix F., 2009. Magnetic particle characterization in the Seine river system: Implications for the determination of natural versus anthropogenic input. Geochem. Geophys. Geosyst., 10, Q08Z05.

Fritz, S.C., 1996. Paleolimnological records of climate change in North America. Limnol. Oceanogr., 41, 882-889.

Gubbins, D., Herrero-Bervera, E., 2007. *Encyclopedia of Geomagnetism and Paleomagnetism*. Springer-Verlag, Berlin, Heidelberg, New York (1054 pp).

Heiri, O., Lotter, A.F., Lemcke, G., 2001. Loss on ignition as a method for estimating organic and carbonate content in sediments: reproducibility and comparability of results. J Paleolimnol. 25(1), 101–110.

Horng, C., Huh, C., Chen, K., Huang, P., Hsiung, K., Lin, H., 2009. Air pollution history elucidated from anthropogenic spherules and their magnetic signatures in marine sediments offshore of Southwestern Taiwan. J. Mar. Syst., 76, 468-478.

Lasheen, M.R., El-Sherif, I.Y., Sabry, D.Y., El-Wakeel, S.T., El-Shahat, M.F., 2015. Adsorption of heavy metals from aqueous solution by magnetite nanoparticles and magnetite-kaolinite nanocomposite: equilibrium, isotherm and kinetic study. Desalin. Water Treat., 57(37), 17421-17429.

Liu, Q., Roberts, A.P., Larrasoaña, J.C., Banerjee, S.K., Guyodo, J., Tauxe, L., Oldfield, F., 2012. Environmental magnetism: Principles and applications. Review of Geophysics, 50, RG4002, DOI:10.1029/2012RG000393.

Maher, B.A., Thompson, R., 1999. Quaternary Climate, Environments and Magnetism. Cambridge University Press, Cambridge, 390 pp.

Matschullat J., Ottenstein R., Reimann C., 2000. Geochemical background – can we calculate it? Environ. Geol., 39 (9): 990–1000.

Mason, R,P. 2013. Trace Metals in Aquatic Systems. Wiley-Blackwell. 431 pp.

Mejia-Echeverry, D.; Chaparro, M.A.E.; Duque-Trujillo, J.F.; Restrepo, J.D., 2018. An environmental magnetism approach to assess impacts of land-derived sediment disturbances on coral reef ecosystems (Cartagena, Colombia). Mar. Pollut. Bull., 131:441–452.

Mendoza-Amézquita, E., Armienta-Hernández, M. A., Ayora, C., Soler, A., Ramos-Ramírez, E., 2006. Potencial lixiviación de elementos traza en jales de las minas La Asunción y Las Torres, en el Distrito Minero de Guanajuato. México. Rev. Mex. Cienc. Geol., 23(1), 75–83.

Metcalfe, S., O'Hara, S., 2000. Sensibilidad de lagos mexicanos a alteraciones en el medio ambiente: ejemplos del Eje Neovolcánico. Ingeniería Hidráulica en México, 7, 107-121.

Miranda-Avilés, R., Puy-Alquiza, M.J., Caudillo-González, M., 2009. Evidencias estratigráficas y geoquímicas de la variación temporal de sedimentos naturales y antropogénicos en la planicie aluvial del río Guanajuato. Rev. Mex. Cienc. Geol., 26(3), 564-574.

Miranda-Avilés, R., Puy-Alquiza, M.J., Pérez Arvizu, O., 2012. Anthropogenic metal content and natural background of overbank sediments from the mining district of Guanajuato, Mexico. Soil. Sediment. Contam., 21, 604–624.

Morton-Bermea, O., Carrillo-Chavez, A., Hernandez, E., & Gonzalez-Partida, E., 2004. Determination of metals for leaching experiments of mine tailings: evaluation of the potential environmental hazard in the Guanajuato mining district, Mexico. Bull. Environ. Contam. Toxicol., 73(4), 770-776.

Pan, Y., Fleet, M., 1991. Barian felsdpar and Barian-Chromian muscovite from the Hemlo area, Ontario. Can. Mineral., 29, 481-498.

Pan, H., Lu, X., Lei, K., Shi, D., Ren, C., Yang, L., Wang, L., 2019. Using magnetic susceptibility to evaluate pollution status of the sediment for a typical reservoir in northwestern China. Environ. Sci. Pollut. Res., 26, 3019-3032. https://doi.org/10.1007/s11356-018-3844-7.

Peters, C., Dekkers., M., 2003. Selected room temperature magnetic parameters as a function of mineralogy, concentration and grain size. Phys. Chem. Earth, 28, 659-667.

Petrovský, E., Kapicka, A., Zapletal, K., Sebestová, E., Spanilá, T., Dekkers, M.J., Rochette, P., 1998. Correlation between magnetic properties and chemical composition of lake sediments from northern Bohemia. Preliminary study. Phys. Chem. Earth, A 23 (9–10), 1123-1126.

R Core Team, 2017. R: A language and environment for statistical computing. R Foundation for Statistical Computing, Vienna, Austria. R version 3.4.0. URL http://www.R-project.org/

Ramos-Arroyo, Y.R., Prol-Ledesma, R.M., Siebe-Grabach, C.D., 2004. Características geológicas y mineralógicas e historia de extracción del Distrito de Guanajuato, México;

Posibles escenarios geoquímicos para los residuos mineros: Rev. Mex. Cienc. Geol., 21(2), 268-284.

Ramos-Arroyo, Y.R., Siebe-Grabach, C.D., 2006. Estrategia para identificar jales con potencial de riesgo ambiental en un Distrito Minero: Estudio de caso en el Distrito de Guanajuato, México. Rev. Mex. Cienc. Geol., 23(1), 54–74.

Ramos-Ramírez, R.E. 1991. Reconstrucción mineralógica de los jales de Guanajuato y el estudio sobre el seguimiento de las especies químicas contenidas en sus componentes no metálicos, Guanajuato. M.Sc. thesis, University of Guanajuato, Mexico.

Roberts, A.P., Chang, L., Rowan, C.J., Horng, C.-S., Florindo, F., 2011. Magnetic properties of sedimentary greigite (Fe_3S_4): an update. Reviews of Geophysics, 10.1029/2010RG000336.

Rose, A. W., Bianchi-Mosquera, G. C., 1993. Adsorption of Cu, Pb, Zn, Co, Ni and Ag on goethite and hematite: a control on metal mobilization from red beds into stratiform copper deposits. Econ. Geol., 88, 1226–36.

Rudnick , R.L., Gao, S., 2003. Composition of the Continental Crust. In D. H. Holland & K. K. Turekian (Eds.), Treatise on Geochemistry (pp. 1-64). Amsterdam, The Netherlands: Elsevier.

Sepúlveda, L.D.; Lecomte, K.L.; Pasquini, A.I.; Mansilla, E.G.; Chaparro, M.A.E., 2019. Propiedades geoquímicas y magnéticas de sedimentos como indicadores de contaminación. Caso de estudio: Río Suquía, Córdoba, Argentina ["Geochemical and magnetic properties of sediments as pollution indicators. Case study: Río Suquía, Córdoba, Argentina"]. Rev. Mex. Cienc. Geol., 36 (2): 183-194.

Servicio Geológico Mexicano, 2017. Cartografía Geoquímica escala 1:250,000. https://datos.gob.mx/busca/dataset?tags=sedimento+de+arroyo, Accessed date: 8 July 2019.

Servicio Meteorológico Nacional (SMN). https://smn.conagua.gob.mx/es/. Accessed date: 10 May 2019.

Singh, B.R., Steinnes, E., 1994. Soil and water contamination with heavy metals. In Soil Proc. Water Quality, Ed. R. Lal & B. A. Stewart, pp. 233–271. Boca Raton, USA: Lewis Publ., CRC Press.

Sutherland, R., 2000. Bed sediment-associated trace metals in an urban stream, Oahu, Hawaii. Environ. Geol., 39 (6), 611-627.

Szefer P., 1998. Distribution and behavior of selected heavy metals and other elements in various components of the southern Baltic ecosystem. Appl. Geochem., 13, 287-292.

Tomlinson DL, Wilson JG, Harris CR, Jeffrey DW, 1980. Problems in the assessment of heavy metals levels in estuaries and the formation of a pollution index. Helgol. Meeresunters, 33, 566-575.

U.S. EPA, 2000. Method 6010C (SW-846): Inductively Coupled Plasma-Atomic Emission Spectrometry, Revision 3. Washington, DC.

U.S. EPA, 2007. Method 3051A (SW-846): microwave assisted acid digestion of sediments, sludges, and soils, Revision 1. Washington, DC.

von der Heyden, B.P., Roychoudhury, A.N., 2015. Application, Chemical Interaction and Fate of Iron Minerals in Polluted Sediment and Soils. Curr. Pollution Rep., 1, 265-279. https://doi.org/10.1007/s40726-015-0020-2

Yang, T., Liu Q., Chan L., Liu Z., 2007. Magnetic signature of heavy metal pollution of sediments: case study from the East Lake in Wuhan, China. Environ. Geol., 52, 1639-1650.

Walden J., Olfield, F., Sdmith, J.P. (eds.), 1999. Environmental Magnetism: a practical guide. Technical Guide, No. 6. Quaternary Research Association, London (243 pp).

Wetzel, R.G., 2001. Limnology. Lake and River Ecosystems. New York. Academic Press (1006 pp).

Zahra, A., Hashmi, M.Z., Malik, R.N., Ahmed, Z., 2014. Enrichment and geo-accumulation of heavy metals and risk assessment of sediments of the Kurang Nallah-Feeding tributary of the Rawal Lake Reservoir, Pakistan. Sci. Total Environ., 470-471, 925-933.

Zhang WG, Yu LZ, Lu M, Hutchinson SM, Feng H., 2007. Magnetic approach to normalizing heavy metal concentrations for particle size effects in intertidal sediments in the Yangtze Estuary, China. Environ. Pollut., 147:238–44.

Zhang, C., Qiao, Q., Piper, J.D.A., Huang, B.B., 2011. Assessment of heavy metal pollution from a Fe-smelting plant in urban river sediments using environmental magnetic and geochemical methods. Environ. Pollut., 59, 3057-3070.

Table and figure captions

Table 1. Geochemical (n=14) and magnetic (n=12) parameters of Guanajuato Hydrological Basin sediments (GHB). Underlined data (SGM-#) were provided by the Servicio Geológico Mexicano (2017).

Table 2. Magnetic, geochemical and index of Purísima Water Reservoir sediments (PWR, n=17).

Fig. 1. Location of the study area in Guanajuato state (México). Green points indicate the sampling sites (CLM-#) of the sediments in the GHB, black triangles correspond to available data provided by the Servicio Geológico Mexicano (SGM-#; Servicio Geológico Mexicano, 2017), and black points show sampling sites (P-#) in the Purísima Water Reservoir, as well as the lithology, land uses and principal tributaries. Red line corresponds to the Mother Lode forming part of the Guanajuato Mining District (GMD).

Fig. 2. Representation of descriptive statistics of magnetic and elements variables for GHB and PWR sediments. The box delineates interquartile range 25−75%, and the horizontal line in box indicates the median. Minimum and maximum values are shown using whiskers, as well as the mean value is shown with an open square.

Fig. 3. Isothermal remanent magnetization measurements and gradient of IRM for (a) a GHB sample, and (b) PWR samples. Two magnetic phases corresponding to magnetite (Comp. 1; $H_{1/2}$= 44.7–57.5mT) and hematite (Comp. 2; $H_{1/2}$= 234.4–457.1mT) were determined.

Fig. 4. (**a**, **c**, **e**) Thermomagnetic (heating run: solid line and cooling run: dash line) and (**b**, **d**, **f**) magnetic hysteresis (magnetization M and adjusted magnetization adj. M are shown with different colors) measurements for GHB and PWR sediment samples.

Fig. 5. SEM observations and elemental quantification by EDS of PWR samples. (**a**, **b**, **c**, **e**) Framboids of pyrite varied from 6-25µm, individual cubo-octahedral crystals are of 1-1.5µm and 0.3-0.5µm. (**d**, **f**) Among magnetic minerals, (titano)magnetite is also observed.

Fig. 6. Enrichment factor EF, enrichment categories (proposed by Sutherland, 2000), and index PLI for GHB and PWR sediment samples are represented. For reference purposes, concentration dependent magnetic parameter χ is displayed. The box delineates interquartile range 25−75%, and the horizontal line in box indicates the median. Minimum and maximum values are shown using whiskers, as well as the mean value is shown with an open square.

Fig. 7. Multivariate analysis of GHB and PWR sediment samples. (**a**) Principal component analysis; (**b**) Representation of the cluster analysis on the principal component map. Three groups were obtained using five PCs, clusters are highlighted in different colors such as cluster 1 in black, cluster 2 in red, and cluster 3 in green color.

Fig. 8. Spatial distribution (built through the ordinary kriging method) of (**a**) mass-specific magnetic susceptibility χ and (**b**) anhysteretic ratio ARM/SIRM of Purísima Water Reservoir sediments. The lowest magnetic concentration (low χ-values) and grain size (high ARM/SIRM-values) are observed in deep water areas, on the contrary, high magnetic concentration and grain size correspond to littoral and river mouth areas. These magnetic proxies (χ and ARM/SIRM) of PTE pollution are directly correlated with Co, Cr, Ni and Pb; and with Ba and P, respectively.

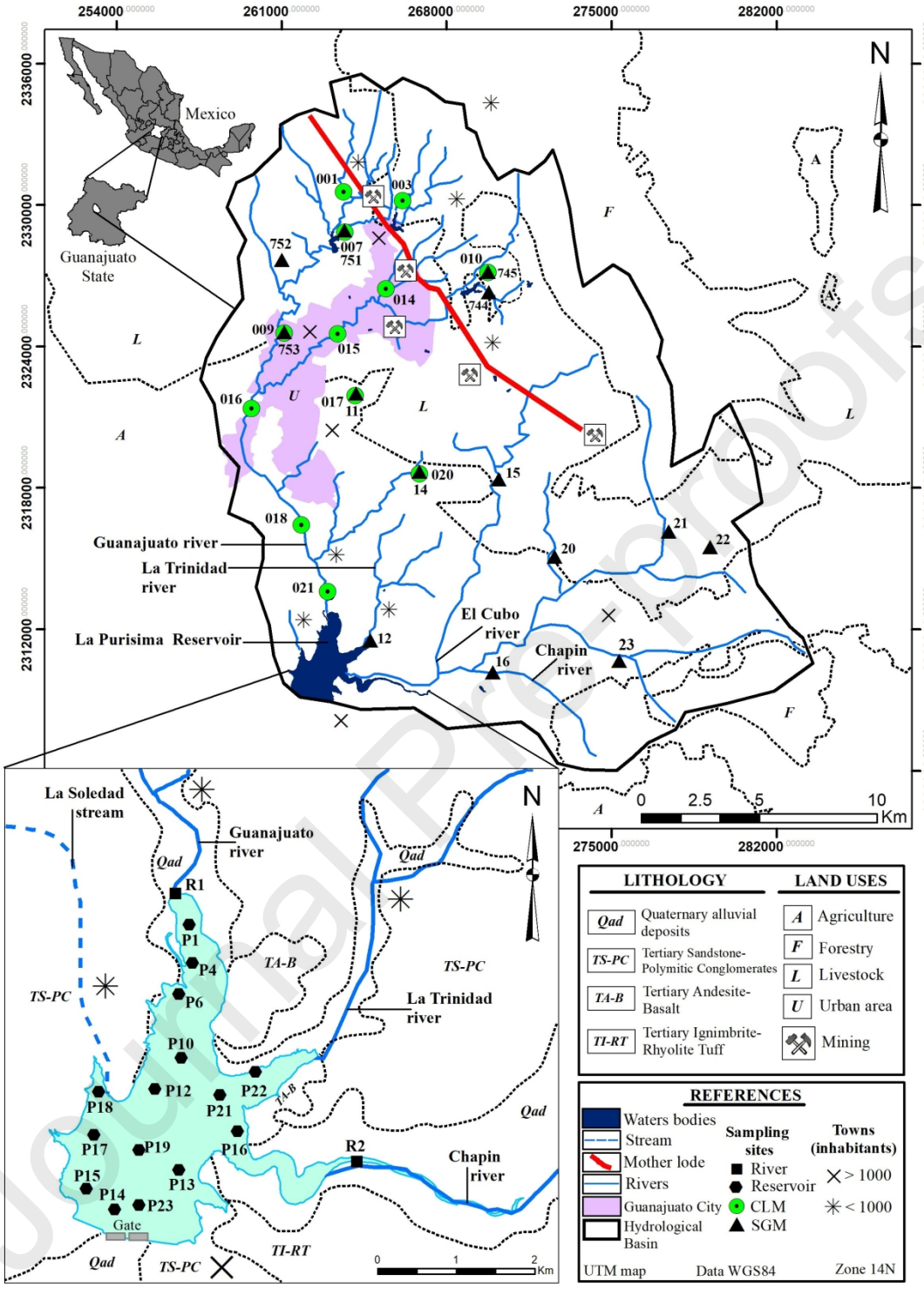

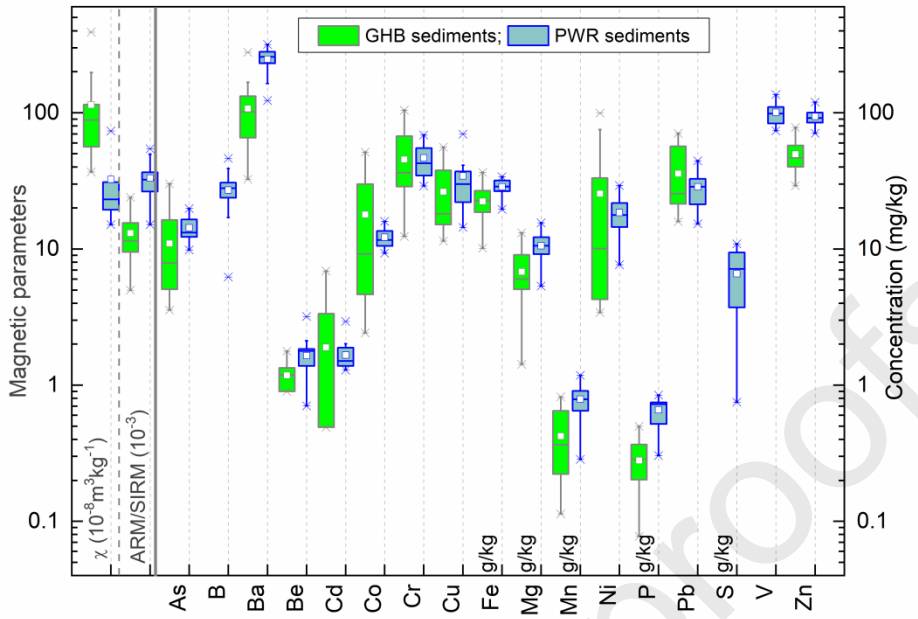

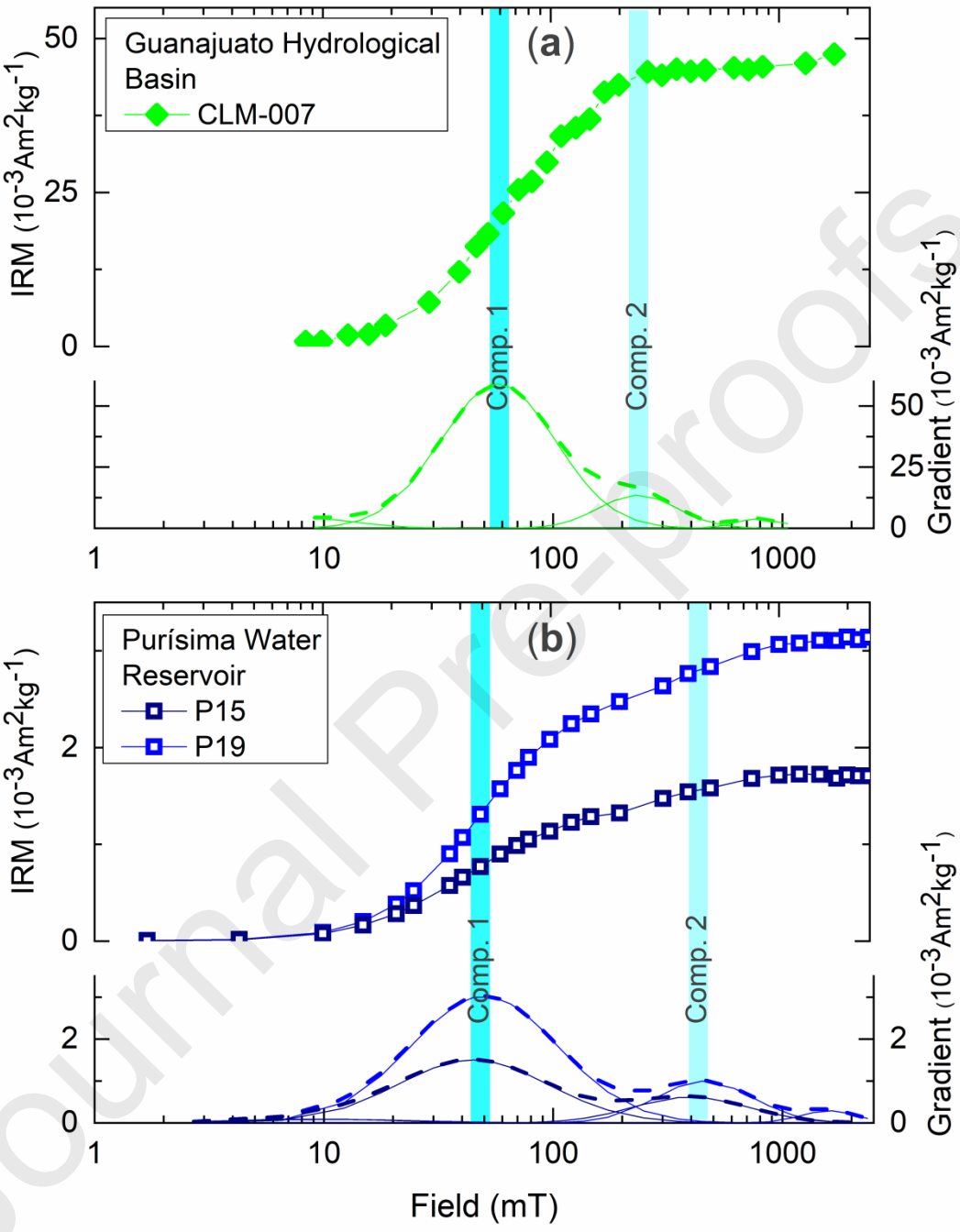

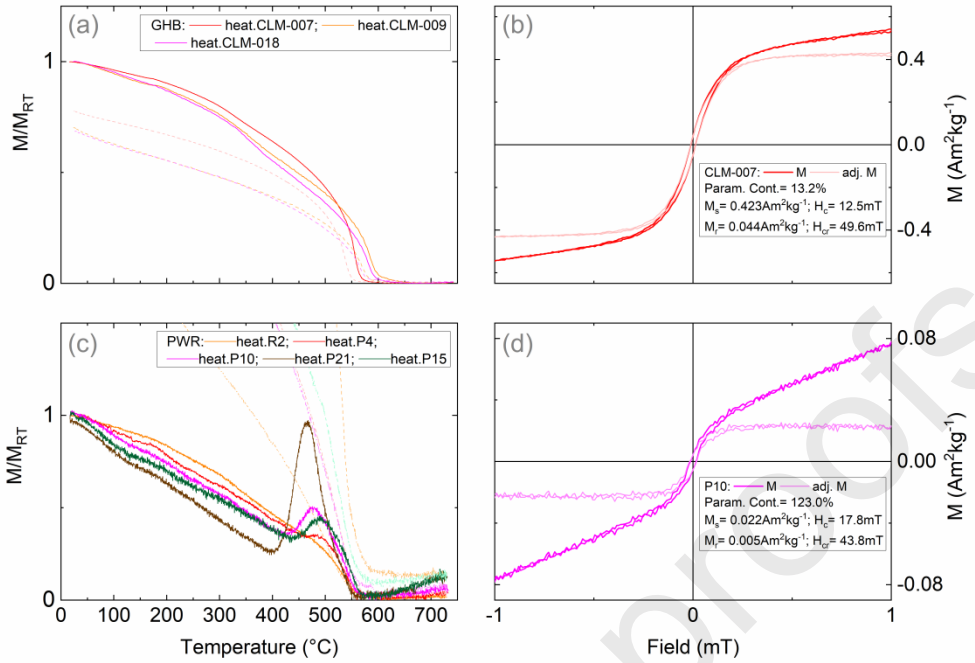

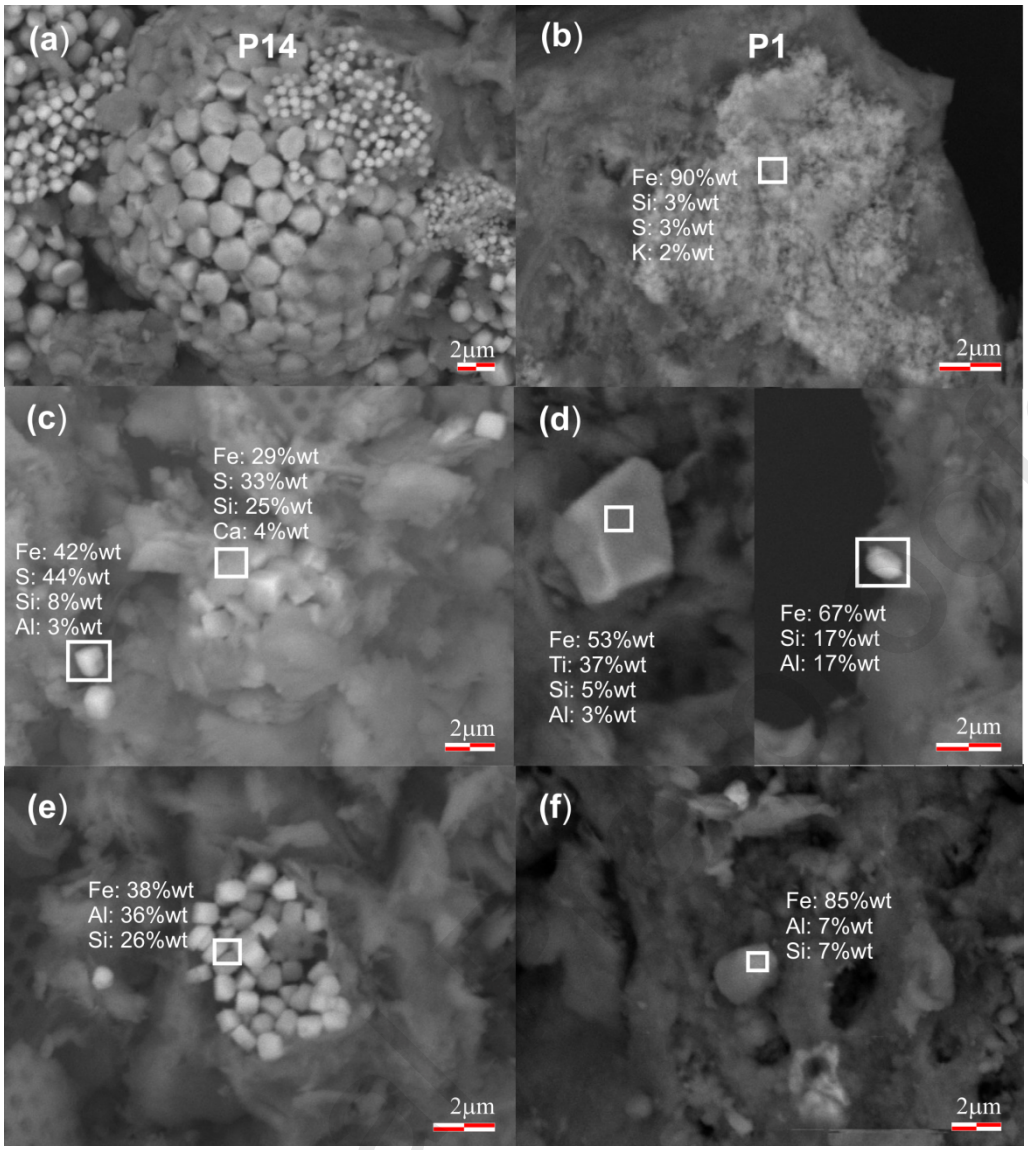

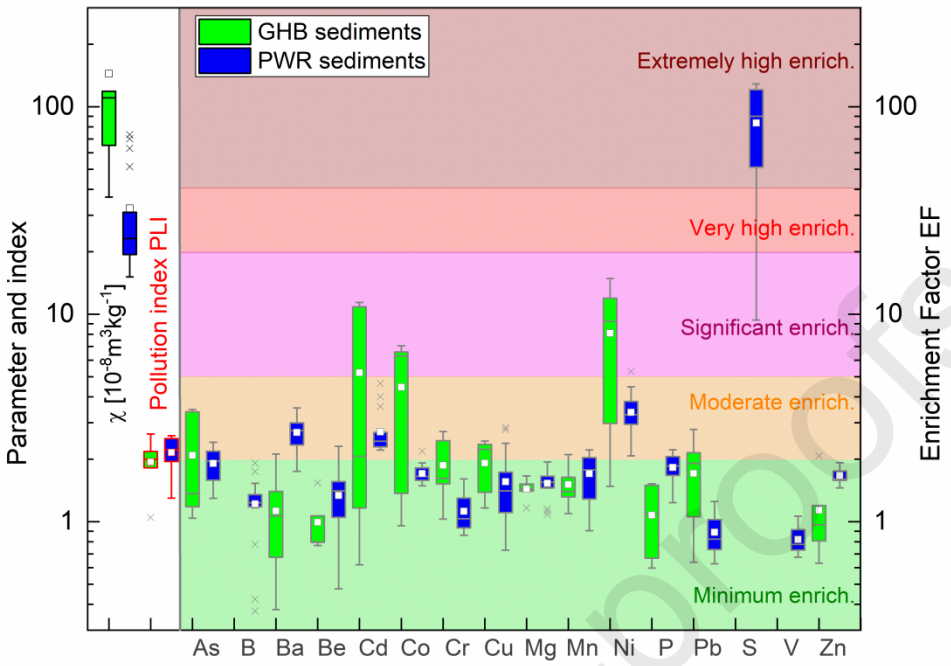

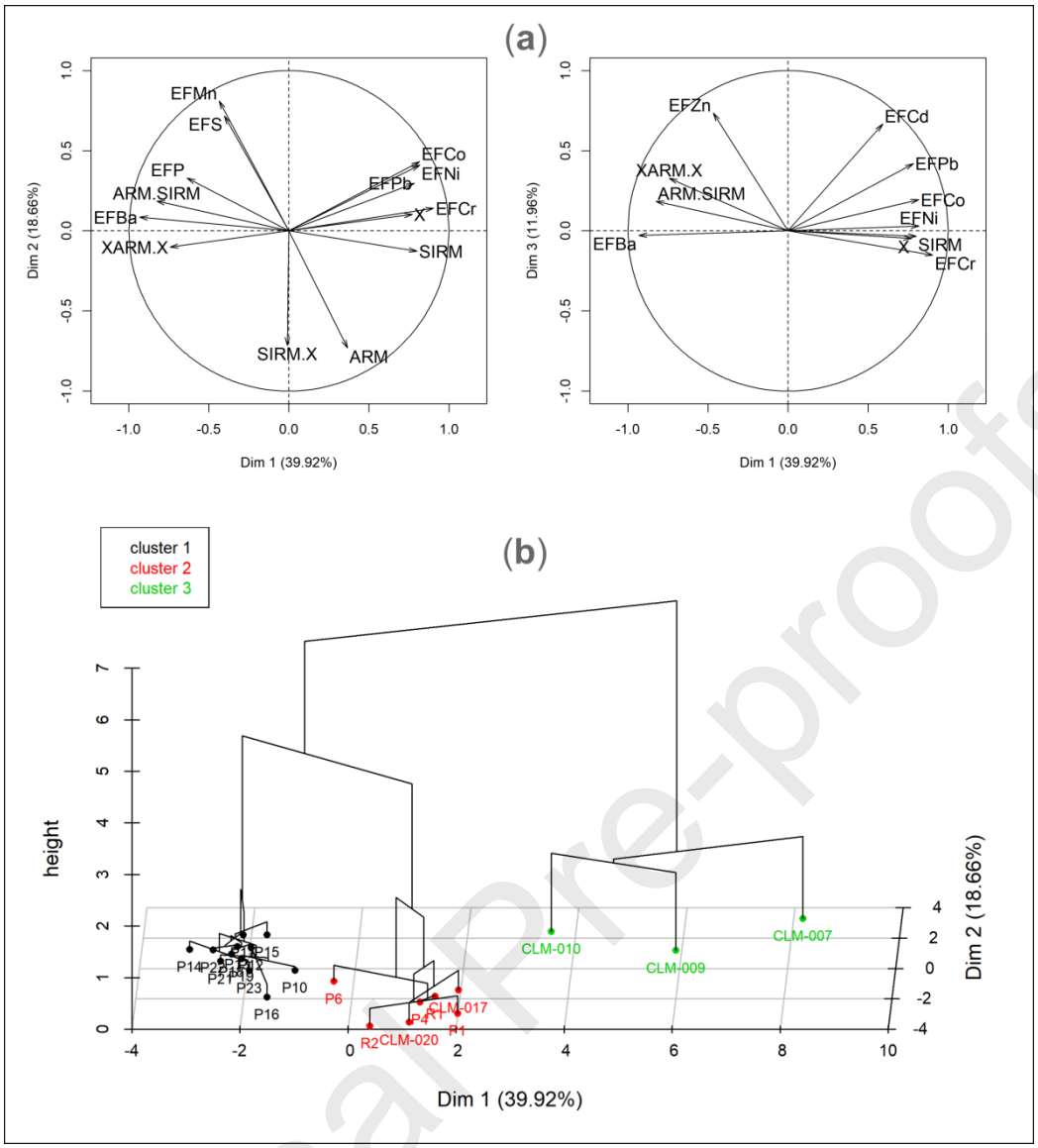

Table 1

Sample	UTM-W	UTM-N	As	Ba	Be	Cd	Co	Cr	Cu	Fe	Mg	Mn
			mg/kg	mg/kg	mg/kg	mg/kg	mg/kg	mg/kg	mg/kg	mg/kg	mg/kg	mg/k
SGM-11	264041	2321919	10.0	164	1.3	0.5	12.5	84.8	37.8	36487	13146	82
SGM-12	264713	2311521	3.6	277	1.3	0.5	6.6	34.4	16.8	18628	4233	29
SGM-14	266825	2318700	6.1	132	1.3	0.5	4.6	28.7	16.9	19426	5363	34
SGM-15	270194	2318334	10.7	104	1.3	0.5	11.1	67.4	27.4	31855	9069	43
SGM-16	269989	2310176	5.9	66	0.9	0.5	3.2	12.4	11.4	12322	1421	13
SGM-20	272563	2315021	6.1	102	1.3	0.5	7.4	42.6	19.3	25044	6495	31
SGM-21	277429	2316135	4.8	131	1.8	0.5	5.7	33.5	15.3	22624	5525	21
SGM-22	279148	2315479	5.1	168	1.6	0.5	4.6	31.4	15.1	22659	5062	22
SGM-23	275386	2310637	4.9	73	1.1	0.5	2.4	14.7	12.8	10142	1602	11
SGM-744	269815	2326280	16.3	101	0.9	3.4	22.4	38.0	14.3	15557	5100	38
SGM-745	269738	2327127	17.1	65	0.9	4.7	30.0	41.7	31.8	19079	6500	64
SGM-751	263724	2328956	23.4	55	0.9	6.0	42.0	89.9	44.9	25502	8500	67
SGM-752	261023	2327612	30.1	34	0.9	6.9	51.4	12.4	56.1	27541	12600	74
SGM-753	261109	2324586	9.7	33	0.9	1.2	47.2	104.7	49.0	26818	10560	56
Background values			*6.0*	*73*	*1.0*	*0.5*	*5.7*	*32.5*	*16.9*	*22624*	*5363*	*36*

Table 2

Sample	UTM-W	UTM-N	χ 10^{-8} m^3 kg^{-1}	SIRM 10^{-3} A m^2 kg^{-1}	ARM 10^{-6} A m^2 kg^{-1}	χ_{ARM} 10^{-8} m^3 kg^{-1}	χ_{FD} 10^{-8} m^3 kg^{-1}	χ_{ARM}/χ a.u.	ARM/SIRM a.u.
P1	263175	2312932	70.1	12.5	260.8	335.8	3.2	4.8	0.021
P4	262929	2312549	63.1	11.7	296.7	370.3	1.5	5.9	0.025
P6	262908	2312040	28.9	6.0	190.4	229.6	1.8	7.9	0.032
P10	262930	2311220	27.2	4.8	190.2	231.2	1.1	8.5	0.039
P12	262604	2310779	18.0	2.5	89.6	100.5	2.3	5.6	0.036
P13	262948	2309758	20.9	3.2	108.3	118.8	0.4	5.7	0.034
P14	262222	2309282	23.2	3.4	184.2	233.7	1.8	10.1	0.054
P15	261774	2309537	15.1	1.7	45.6	60.9	0.6	4.0	0.026
P16	263677	2310281	28.6	6.0	192.7	237.7	1.3	8.3	0.032
P17	261852	2310234	19.4	2.5	72.9	87.0	0.7	4.5	0.029
P18	261925	2310782	31.0	4.5	136.5	162.0	1.4	5.2	0.031
P19	262402	2310031	19.0	3.1	140.6	169.4	0.9	8.9	0.045
P21	263446	2310739	20.3	4.2	146.2	173.4	0.4	8.5	0.035
P22	263882	2311056	19.3	2.8	100.9	119.8	0.8	6.2	0.037
P23	262401	2309318	21.2	3.4	171.0	206.4	1.5	9.8	0.050
R1	262861	2313127	73.4	12.6	277.5	358.8	1.5	4.9	0.022
R2	265055	2310134	51.5	13.3	201.7	263.8	2.7	5.1	0.015

Background values

Background values were calculated using 14 GHB samples (Servicio Geológico Mexicano SGM, 2017) and the iterative 2-δ te

Highlights

- Magnetic parameters as proxies for element pollution in water reservoirs.
- Element contamination is mainly associated with historical mining activities.
- Iron oxides and iron sulfides are detected and characterized in water reservoir sediments.
- Multivariate analysis for magnetic and enrichment variables shows differences between reservoir and basin sediments.